

**An empirical algorithm to estimate spectral average cosine of underwater light field from remote sensing data in coastal oceanic waters**

Madhubala Talaulikar<sup>1</sup>, T Suresh<sup>1</sup>, Elgar Desa<sup>1</sup>, A. Inamdar<sup>2</sup>,

<sup>1</sup> National Institute of Oceanography, Goa, India, 403004

<sup>2</sup> Indian Institute of Technology Bombay, Mumbai, India, 400076

**Abstract**

The underwater average cosine is an apparent optical property of water that describes the angular distribution of radiance at a given point in water. Here we present a simple empirical algorithm to estimate spectral underwater average cosine  $\bar{\mu}(\lambda)$  where the wavelength  $\lambda$  ranges from 400 nm to 700 nm, based only on the apparent optical property, remote sensing reflectance,  $R_{rs}(\lambda)$  and solar zenith angle. The algorithm has been developed using the measured optical parameters from the coastal waters off Goa, India and eastern Arabian Sea and the optical parameters derived using the radiative transfer code using these measured data. The algorithm was compared with two earlier reported empirical algorithms of Haltrin (1998, 2000) and the performance of the algorithm was found to be better than these two empirical algorithms. The algorithm is based on single optical parameter; remote sensing reflectance which can be easily measured *in-situ* and is available from the ocean color satellite sensors, hence this algorithm will find applications in the ocean color remote sensing.

## Introduction

Understanding the underwater light field in coastal waters and other shelf seas is important for the study of marine bio-optics. Underwater light field depends on the optical characteristics of the seawater and the conditions of illumination. The behavior of the underwater light field is described by the radiative transfer equation and this equation relates the underwater light field to the inherent optical properties of water and its constituents (Zaneveld 1989). Radiance and Irradiance are the two fundamental optical properties used to describe the underwater light field. The radiance ( $L(\lambda)$ ) and scalar ( $E_o(\lambda)$ ) and planar ( $E(\lambda)$ ) irradiances introduces new optical property that is used to describe the underwater light field called underwater average cosine with its three components: total underwater average cosine ( $\bar{\mu}(\lambda)$ ), underwater average cosine for downwelling light field ( $\bar{\mu}_d(\lambda)$ ) and underwater average cosine for upwelling light field ( $\bar{\mu}_u(\lambda)$ ). The three average cosines are defined mathematically as given in Equation 1, 2 and 3 respectively (Berwald 1998, Mobley, 1994).

$$\bar{\mu}(z, \lambda) = \frac{\int_0^{2\pi} \int_0^{\pi} L(z, \lambda, \theta, \phi) \cos \theta \sin \theta d\theta d\phi}{\int_0^{2\pi} \int_0^{\pi} L(z, \lambda, \theta, \phi) \sin \theta d\theta d\phi} = \frac{E_d(z, \lambda) - E_u(z, \lambda)}{E_o(z, \lambda)} \quad (1)$$

$$\bar{\mu}_d(z, \lambda) = \frac{\int_0^{2\pi} \int_0^{\frac{\pi}{2}} L(z, \lambda, \theta, \phi) \cos \theta \sin \theta d\theta d\phi}{\int_0^{2\pi} \int_0^{\frac{\pi}{2}} L(z, \lambda, \theta, \phi) \sin \theta d\theta d\phi} = \frac{E_d(z, \lambda)}{E_{od}(z, \lambda)} \quad (2)$$

$$\bar{\mu}_u(z, \lambda) = \frac{\int_0^{2\pi} \int_{\frac{\pi}{2}}^{\pi} L(z, \lambda, \theta, \phi) \cos \theta \sin \theta d\theta d\phi}{\int_0^{2\pi} \int_{\frac{\pi}{2}}^{\pi} L(z, \lambda, \theta, \phi) \sin \theta d\theta d\phi} = \frac{E_u(z, \lambda)}{E_{ou}(z, \lambda)} \quad (3)$$

where  $E_d(z, \lambda)$ ,  $E_u(z, \lambda)$ ,  $E_d(z, \lambda) - E_u(z, \lambda)$  and  $E_o(z, \lambda)$  are the spectral downwelling irradiance, upwelling irradiance, net irradiance and scalar spectral irradiance at depth  $z$  and wavelength  $\lambda$ . The underwater average cosine varies spectrally and with depth, hence for brevity the depth is not indicated. The underwater average cosine for the entire light field can also be defined as the average cosine of zenith angles of all the photons at a particular point (Kirk 1994; Mobley 1994; Berwald et al. 1995).

Since the average cosine gives directional information about the radiance distribution, it varies between 0 and 1, with value of  $\bar{\mu}(\lambda) = 0$  indicating that light is uniformly distributed in the water and when  $\bar{\mu}(\lambda) = 1$  all the light is propagating vertically down. The value of  $\bar{\mu}(\lambda)$  depends on the absorption and scattering properties of the medium (Kirk 1981; Bannister 1992), thus it is higher in absorption-dominated waters such as Open Ocean than in coastal waters. The  $\bar{\mu}(\lambda)$  decreases with depth and the rate of change with depth for most waters is strongly dependent on scattering, while influence of absorption is only seen in clear waters (Berwald et al. 1995). Though the value of  $\bar{\mu}(\lambda)$  varies with the inherent optical properties of water, it is often assumed to be a constant value in ecosystem models. For example Penta et al (2008) assumes the value of  $\bar{\mu}(\lambda)$  as 0.7 to study the effect of light schemes on an ecosystem model causing negligible error. Ciotti et al. (1999) also assumes the value of  $\bar{\mu}(\lambda)$  as 0.7 for developing a model to examine the influence of phytoplankton community structure on the relationship between diffuse attenuation and ratios of upwelling radiance. However, Sathyendranath and Platt (1989) state that the angular distribution of light has to be considered while estimating the primary productivity and neglecting this factor can lead to underestimation of primary productivity. Other factors that influences the underwater average cosine includes sea surface conditions, the incident illumination at the sea surface, phase function of scattering (McCormick 1995), scattering (Berwald et al. 1995).

Stramska et al. (2000) modeled  $\bar{\mu}(\lambda)$  in terms of  $E_d(z, \lambda)$ ,  $E_u(z, \lambda)$  and  $L_u(z, \lambda)$  for the blue green spectral region. Berwald et al. (1995) also developed a model for deriving underwater average cosine in terms of absorption and scattering coefficient. However, this model was developed only for optically homogeneous waters having Petzold (Petzold 1972) scattering phase function. Models are also available for calculating depth profiles of underwater mean cosine (Zaneveld 1989; Bannister 1992; Berwald et al. 1995). Preisendorfer (1959) and Hojerslev and Zaneveld (1977) demonstrated that the theoretically modeled average cosine decays exponentially with depth (Zaneveld 1989) and approaches an asymptotic state at sufficiently greater depth. All these studies were limited to homogenous waters. Kirk (1981) used variations in average cosine as a function of optical depth at a given scattering to absorption ratio to model the penetration of light in water.

Hojerslev (1973) developed an absorption meter with two collectors that measured scalar and vector irradiances simultaneously from which the average cosine could be derived. Presently there is no commercial instrument available that can directly measure average cosine for underwater light field. The

only reported empirical algorithms by Haltrin (1998) and Haltrin (2000) using the experimental data measured by Timofeyeva (1971) to determine underwater average cosine require inherent optical properties like absorption, scattering, beam attenuation and back scattering which themselves are difficult to measure. These two algorithms will be hereafter referred as Haltrin and Timofeyeva respectively. Despite its importance, no extensive work has been carried out to estimate the spectral underwater average cosine from ocean color remote sensing satellite sensors. The algorithms of Haltrin and Timofeyeva require inherent optical properties and hence to derive  $\bar{\mu}(\lambda)$  from ocean color data, it is first required to obtain these optical parameters using empirical algorithms. An empirical algorithm developed by Talaulikar et al. (2012) based only on the remote sensing reflectance could be used to derive  $\bar{\mu}(490)$  from the ocean color satellite data. This algorithm performed better than those of Haltrin and Timofeyeva at 490nm. Probable reasons could be due to errors in the inherent optical properties estimated using empirical relationships; remote sensing reflectance derived from the ocean color satellite data and also to the formulation of the simple algorithm based on the value of remote sensing reflectance. To demonstrate the utility value of the algorithm developed by Talaulikar et al. 2012,  $\bar{\mu}(490)$  was used to estimate the absorption coefficient  $a(490)$  and the validation of  $a(490)$  derived using this algorithm with the NOMAD and IOCCG data sets showed very close match (Talaulikar et al. 2012).

Here we present an empirical algorithm to estimate spectral underwater average cosine for the wavelengths ranging from 400 nm to 700 nm. The algorithm is based on the ratio of remote sensing reflectance and thus could be used to derive underwater average cosine from ocean color satellite data. It also considers the effect of solar zenith angle. The algorithm however cannot be used to derive the depth profile of underwater average cosine.

#### Notation

$\bar{\mu}$	Underwater average cosine
$\bar{\mu}_u$	Underwater average cosine for upwelling light field
$\bar{\mu}_d$	Underwater average cosine for downwelling light field
$R_{rs}$	Remote sensing reflectance ( $\text{sr}^{-1}$ )
$E_d$	Downwelling irradiance ( $\text{watts/m}^2$ )
$E_u$	Upwelling irradiance ( $\text{watts/m}^2$ )
$E_0$	Scalar irradiance ( $\text{watts/m}^2$ )
$E_{od}$	Scalar downward irradiance ( $\text{watts/m}^2$ )
$E_{ou}$	Scalar upward irradiance ( $\text{watts/m}^2$ )

$a$	Absorption coefficient ( $\text{m}^{-1}$ )
$b$	Scattering coefficient ( $\text{m}^{-1}$ )
$c$	Beam attenuation coefficient ( $\text{m}^{-1}$ )
$b_b$	Back scattering coefficient ( $\text{m}^{-1}$ )
$K_d$	Diffuse attenuation coefficient for downwelling irradiance ( $\text{m}^{-1}$ )
$K_E$	Diffuse attenuation coefficient for net irradiance ( $\text{m}^{-1}$ )
$\omega_0$	Single scattering albedo
$\theta$	Solar zenith angle (radians)
$\varphi$	Azimuth angle (radians)
$\Omega$	Solid angle (radians)
$\lambda$	Wavelength of light (nm)
$Z_{90}$	Penetration depth (First optical depth) (m)
$Z_{sd}$	Secchi Depth (m)
$a_{ac}$	Absorption coefficient measured by AC-9 and corrected for temperature, salinity and scattering effects. ( $\text{m}^{-1}$ )
$c_{ac}$	Beam attenuation coefficient measured by AC-9 and corrected for temperature and salinity errors. ( $\text{m}^{-1}$ )

## Materials and Procedures

### Materials

Instruments AC-9 (Wetlabs Inc.) and HyperOCR hyperspectral radiometer (Satlantic Inc.) were used to measure inherent and apparent optical properties respectively. The instrument AC-9 was calibrated in the laboratory prior to every field measurement using optically clean water, whereas hyperspectral radiometer was factory calibrated. AC-9 provided absorption, and beam attenuation coefficient (without contribution from pure water) at nine wavelengths 412, 440, 488, 510, 532, 555, 650, 676 and 715 nm. The absorption and beam attenuation from AC-9 were corrected for salinity and temperature effects (Pegau et al. 1997) using salinity and temperature measured by the CTD sensors. Absorption data were then corrected for scattering effects using proportionate correction method (Zaneveld 1994). The corrected AC9 absorption and beam attenuation coefficients will be referred as  $a_{ac}(\lambda)$  and  $c_{ac}(\lambda)$  respectively. HyperOCR measured the depth profiles of upwelling radiance ( $L_u(\lambda)$ ) and downwelling irradiance ( $E_d(\lambda)$ ) in water for wavelengths 350 to 800 nm, and the reference sensor of HyperOCR measured surface solar irradiance on the deck. These measurements were carried-out in the coastal waters off Goa (India), estuaries of Mandovi and Zuari (15. 40° N – 15.54 ° N, 73.70 °E – 73.99 °E) of Goa during 2010 and 2011 at 38 stations and during the cruise SSK009 and SSK017 on R.V *Sindhu Sankalp* in the eastern Arabian Sea at 11 stations (Figure 1) for a total of 49 stations. The optical measurements were carried out between 05:30 hrs to 07:30 hrs GMT under fair weather condition.

Maximum water depth varied from 5 to 20 m for estuaries and coastal waters off Goa, whereas it varied from 35 to 840 m in the Arabian Sea. The Secchi depth ( $Z_{sd}$ ) for all stations varied from 2 to 27 m.  $Z_{sd}$  which is an indicator of transparency of water was used as a simplest mean to classify the water types. The solar zenith angle during the measurements varied from  $16.5^\circ$  to  $55.5^\circ$ . The underwater average cosine at 490 nm for the study area varied from 0.5 to 0.9.

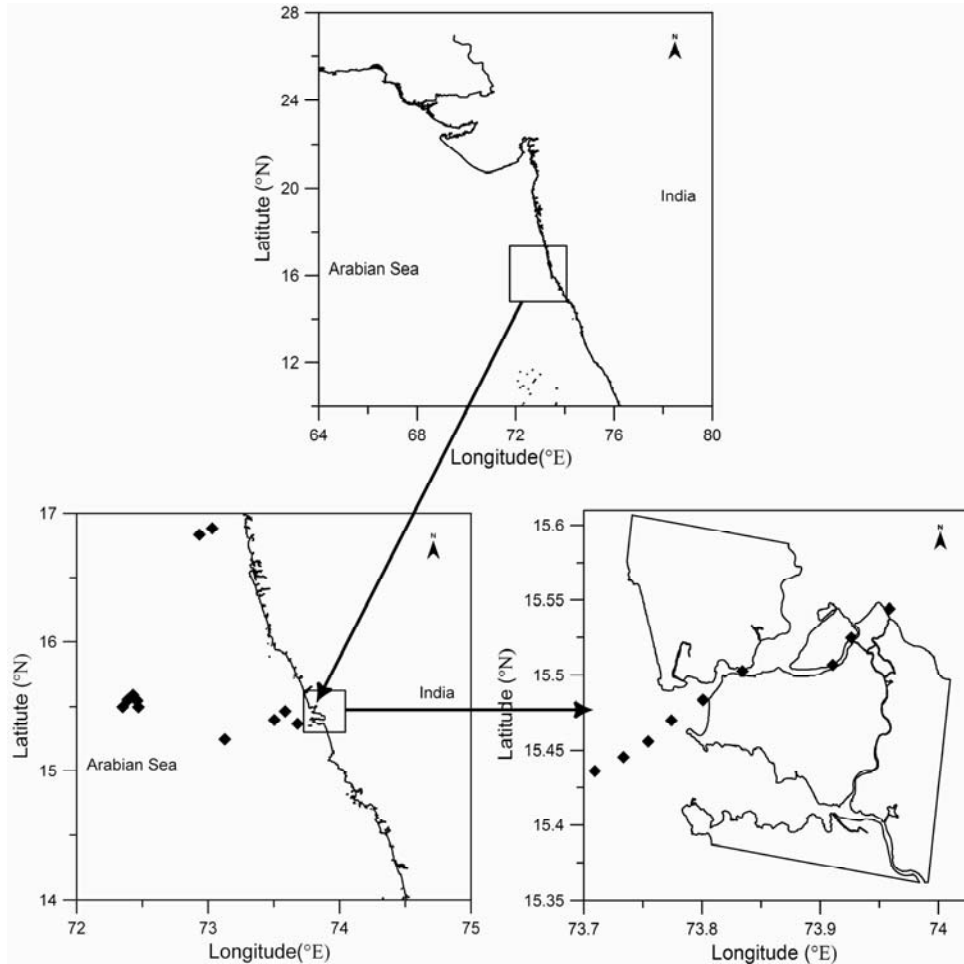


Figure 1. Locations of the optical measurements carried out in Eastern Arabian Sea and coastal waters off Goa

### Algorithm Development

Figure 2 depicts the steps involved in the development of the algorithm and the process is described in detail below. A radiative transfer model Hydrolight version 5.1 (Mobley 1994) was used to simulate the apparent optical properties and also to obtain  $\bar{\mu}(\lambda)$  using equation (1). Simulations using the Hydrolight model were run with inputs,  $a_{ac}(\lambda)$  and  $c_{ac}(\lambda)$ , surface irradiance measured by reference

sensor of the radiometer, HyperOCR, the bottom reflectance derived from the measurements close to the bottom using HyperOCR ( Lee et al. 1999) (assuming that the bottom type is Lambertian type) and the meteorological data such as wind speed and relative humidity available from AWS-NIO, Automatic Weather Station of National Institute of Oceanography, Goa. The simulations were carried out for every 1 nm, and a depth interval of 1 m. All the simulations neglected the effect of inelastic scattering and bioluminescence. Since the measurements of phase function were not available, the optimum Fournier-Forand (FF) phase function was used (Fournier and Forand 1994). The best suited FF phase function for a particular station was selected by first simulating the optical properties using all available depth independent FF phase functions with  $b_b/b$  value ranging from 0.0001 to 5.0 by keeping all other inputs unchanged.  $R_{rs}(\lambda)$  generated by all the Hydrolight runs were then compared against the  $R_{rs}(\lambda)$  measured using radiometer. The FF phase function that generated the best matching  $R_{rs}(\lambda)$  with minimum percentage deviation over the spectral range was selected as the optimum FF phase function for that station. Although depth dependent phase function is required for efficient simulations (Sundarabalan and Shanmugam 2013), it has been reasoned by Mobley et al (2002) that use of depth independent Fournier- Forand phase function provides better results than any other phase function available in Hydrolight. The simulations carried out using the above inputs provided good optical closure between modeled and measured remote sensing reflectance, thus enhancing the confidence in the data derived from the Hydrolight to be used for development of algorithm (See Figure 3).

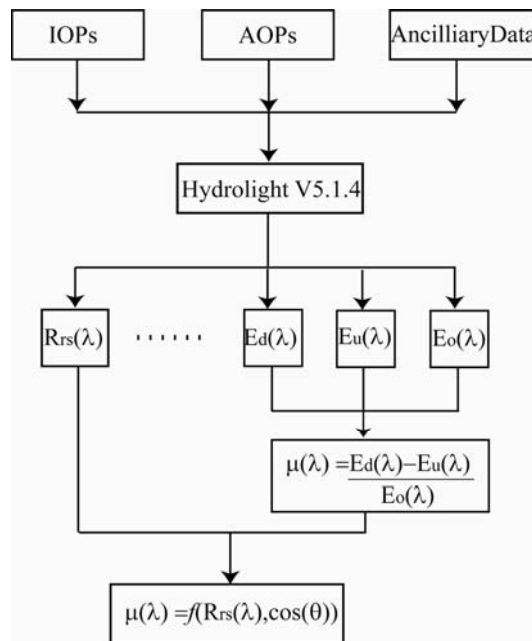


Figure 2. Block diagram showing the steps involved in development of the algorithm

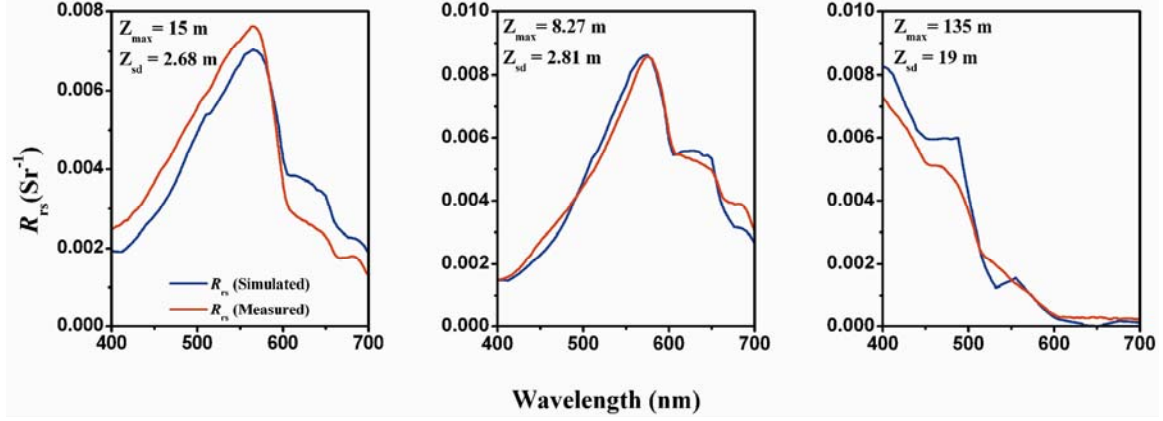


Figure 3. Comparison of remote sensing reflectance generated from Hydrolight simulations and in situ measured using Satlantic HyperOCR for different water types. Here  $Z_{\max}$  is Maximum depth of the station and  $Z_{sd}$  is the Secchi depth.

The average cosine  $\bar{\mu}(\lambda)$  has been reported to be highly correlated with irradiance reflectance and solar zenith angle,  $\theta$  (Pelevin and Prokudina 1979; Kirk 1981; Kirk 1994; Stramska et al. 2000). The following two facts encouraged us to develop the algorithm for deriving spectral underwater average cosine. One, the algorithm developed earlier (Taulikar et al 2012) to derive underwater average cosine at 490nm using  $R_{rs}(490)$  provided good results when compared to the other published algorithms of Haltrin and Timofeyeva and second,  $R_{rs}(\lambda)$ , which is defined as the ratio of upwelling radiance to downwelling irradiance just above the sea surface (Equation 4) is one of the prime optical parameters that is derived from ocean color satellite sensors after applying the appropriate atmospheric correction algorithm. The new algorithm to derive spectral  $\bar{\mu}(\lambda)$  that is based on  $R_{rs}(\lambda)$  and  $\theta$ , will allow us to derive the  $\bar{\mu}(\lambda)$  from the satellite data (Equation 5 and 6). The following simple empirical relationship was developed using  $R_{rs}(\lambda)$ , solar zenith angle,  $\theta$  and  $\bar{\mu}(\lambda)$  generated from Hydrolight simulations.

$$R_{rs}(\lambda) = \frac{L_w(\lambda)in\_air}{E_d(\lambda)in\_air} \quad (4)$$

$$\bar{\mu}(\lambda) = M_0 + M_1 * X + M_2 * X^2 \quad (5)$$

$$X = \frac{R_{rs}(\lambda)}{\log(R_{rs}(620) + R_{rs}(\lambda))} * \frac{1}{\cos(\theta)} \quad (6)$$

where  $M_0$ ,  $M_1$  and  $M_2$  are coefficients of the polynomial and their values at every 10 nm are given in Table 1 and  $\theta$  is the solar zenith angle. Since the algorithm is developed for ocean color satellite applications,  $\bar{\mu}(\lambda)$  used for algorithm development and validation were averaged over the spectral



penetration depth,  $Z_{90}(\lambda)$  where  $Z_{90}(\lambda)$  is defined as  $Z_{90}(\lambda)=1/K_d(\lambda)$  . This  $Z_{90}$  is an important parameter for ocean color remote sensing studies as it defines the depth from which 90% of the contribution of the water leaving radiance emerges to the surface and is detected by the satellite sensor (Gordon and Clark 1980). The algorithm was found to work well normalizing  $R_{rs}$  with  $R_{rs}$  in the red region of 620 nm. Indian ocean color satellite OCM-2 (Ocean Color Monitor-2) has a band at 620 nm and  $\bar{\mu}$  has maximum values in red region of the spectrum. This algorithm to derive spectral  $\bar{\mu}(\lambda)$  will be hereafter referred as Mu.

Table 1 Lookup table of the coefficients of polynomial equation to derive spectral underwater average cosine

Wavelength (nm)	$M_0$	$M_1$	$M_2$
400	0.868	222.642	74070.620
410	0.872	239.009	84124.640
420	0.876	254.457	98398.130
430	0.877	261.646	104304.928
440	0.870	231.856	77259.332
450	0.864	212.429	60000.396
460	0.859	193.097	45444.714
470	0.856	179.786	35496.185
480	0.851	165.740	27247.601
490	0.846	150.084	20314.032
500	0.842	141.779	16486.846
510	0.837	129.438	12769.781
520	0.834	129.724	12099.032
530	0.830	121.877	10320.286
540	0.829	118.116	9542.129
550	0.828	117.243	9420.482
560	0.829	116.041	9218.284
570	0.831	117.326	9430.486
580	0.836	121.766	10470.744
590	0.844	134.301	13721.434
600	0.854	166.286	23608.745
610	0.861	177.430	28875.384
620	0.862	177.150	29266.345
630	0.863	177.997	29943.959
640	0.863	182.343	31918.691
650	0.864	177.047	31352.697
660	0.868	210.854	47065.215
670	0.871	218.601	53650.950
680	0.872	219.721	55900.221
690	0.872	217.200	55714.685
700	0.875	240.049	69855.721

### Evaluation of the algorithm, Mu

The evaluation of the algorithm Mu to determine the spectral underwater average cosine  $\bar{\mu}(\lambda)$  was carried out using the  $R_{rs}(\lambda)$  measured using the hyperspectral radiometer. The algorithm Mu was compared with the other published algorithms of Haltrin and Timofeyeva, listed as equations 7 and 8 respectively.

$$\bar{\mu} = \sqrt{\frac{a}{a + 3b_b + \sqrt{b_b(4a + 9b_b)}}} \quad (7)$$

$$\bar{\mu} = y\{C_0 + y[C_1 + y(C_2 + y\{C_3 + y[C_4 + y(C_5 + C_6y)]\})]\} \quad (8)$$

where

$$y = \sqrt{1 - \frac{b}{c}} \quad (9)$$

$C_0 = 2.6178398$ ,  $C_1 = -4.602418$ ,  $C_2 = 9.00406$ ,  $C_3 = -14.59994$ ,  $C_4 = 14.83909$ ,  $C_5 = -8.117954$ ,  $C_6 = 1.8593222$ .

Error analyses were carried out using the statistical parameters APD (Average Percentile Deviation), MPD (Mean Percentage Deviation), RMSE (Root Mean Square Error), Coefficient of determination ( $R^2$ ) and Relative Difference (RD) and they are defined as below

$$APD = \exp \left[ \text{mean} \left| \ln \left( \frac{\bar{\mu}_{Estimated}}{\bar{\mu}_{Hydrolight}} \right) \right| \right] - 1 \quad (10)$$

$$MPD = \left[ \frac{1}{N} \sum_1^N \frac{(\bar{\mu}_{Estimated} - \bar{\mu}_{Hydrolight})}{\bar{\mu}_{Hydrolight}} \right] \times 100\% \quad (11)$$

$$RMSE = \sqrt{\frac{\sum (\bar{\mu}_{Hydrolight} - \bar{\mu}_{Estimated})^2}{N}} \quad (12)$$

$$RD = \frac{\bar{\mu}(\lambda)_{Estimated} - \bar{\mu}(\lambda)_{Hydrolight}}{\bar{\mu}(\lambda)_{Hydrolight}} \quad (13)$$

where N is the total number of data analyzed,  $\bar{\mu}_{Estimated}$  is the underwater average cosine derived using proposed algorithm Mu and  $\bar{\mu}_{Hydrolight}$  is underwater average cosine obtained from the Hydrolight simulations.

The inter-comparison of algorithms Mu, Haltrin and Timofeyeva were carried out using the measured  $R_{rs}(\lambda)$  and the values of  $\bar{\mu}(\lambda)$  derived from these algorithms were compared with those derived from the Hydrolight simulations (Figure 4). The objective of using the  $R_{rs}(\lambda)$  for all the

algorithms was to determine the most suitable algorithm for deriving  $\bar{\mu}(\lambda)$  from the ocean color satellite data. Values of  $a(\lambda)$  and  $b_b(\lambda)$  required for calculating  $\bar{\mu}(\lambda)$  using algorithm of Haltrin were derived using the updated algorithm QAA Version 5(Quasi Analytical Algorithm)(Lee et al. 2002, 2007). Algorithm QAA derives absorption and back scattering coefficient by analytically inverting the spectral remote sensing reflectance. This algorithm produces better results for deriving spectral total absorption coefficient and backscattering coefficients (Qin et al. 2007; Shanmugam et al, 2010). However, its performance is poor for deriving components of absorption (Shanmugam et al. 2010). Though  $b(\lambda)$  is required for algorithm of Timofeyeva, it is seldom derived from the satellite data as the contribution to the water leaving radiance is mostly from the backscattering coefficient. There are few algorithms to derive  $b(\lambda)$ . The method by Gallegos and Corell (1990) assume that the absorption at 720 nm to be only from pure water and zero from all other sources such as CDOM and phytoplankton, which may not be valid for all waters and the  $b$  derived using this algorithm is assumed to

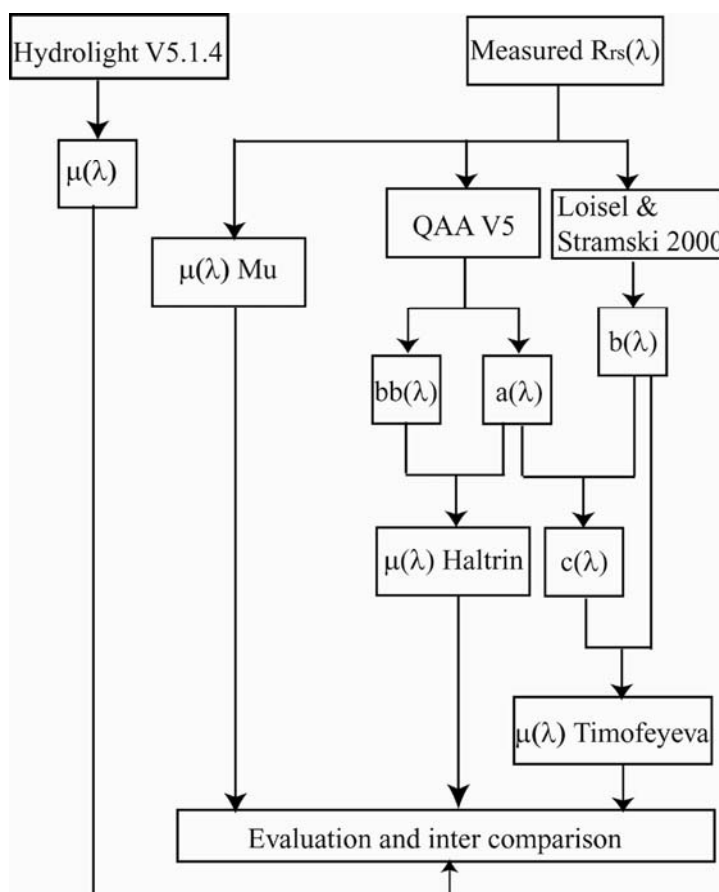


Figure 4. Schematic of steps involved in evaluation of algorithm Mu using in-situ measured remote sensing reflectance.

be spectrally invariant. Another empirical algorithm use  $b(555)$  to derive spectral  $b(\lambda)$  (Gould et al. 1999, 2001). An empirical relationship based on chlorophyll is more suited for Case 1 waters (Gordon and Morel, 1983). The other models by Kopelevich and Haltrin are based on volume concentrations of small and large particles (Mobley 1994). Considering the application and ease of use, the model by Loisel and Stramski (2000) was chosen for this study as all the parameters used could be derived from the ocean color satellite data.

The algorithms were evaluated in four spectral regions, Visible or PAR (400nm – 700nm), Blue (400nm – 500nm), Green (500nm - 600nm) and Red (600nm - 700nm) regions.

## Results

### *Spectral underwater average cosine for different water types*

The underwater average cosine  $\bar{\mu}(\lambda)$  varied with various water types. Values of  $\bar{\mu}(\lambda)$  were low for very turbid waters whereas they were higher for relatively clear waters (Figure 5). Similar spectral variations of  $\bar{\mu}(\lambda)$  were also reported by Berwald et al. (1998). It shows lower values of  $\bar{\mu}(\lambda)$  for coastal turbid waters as compared to that for relatively clearer waters.

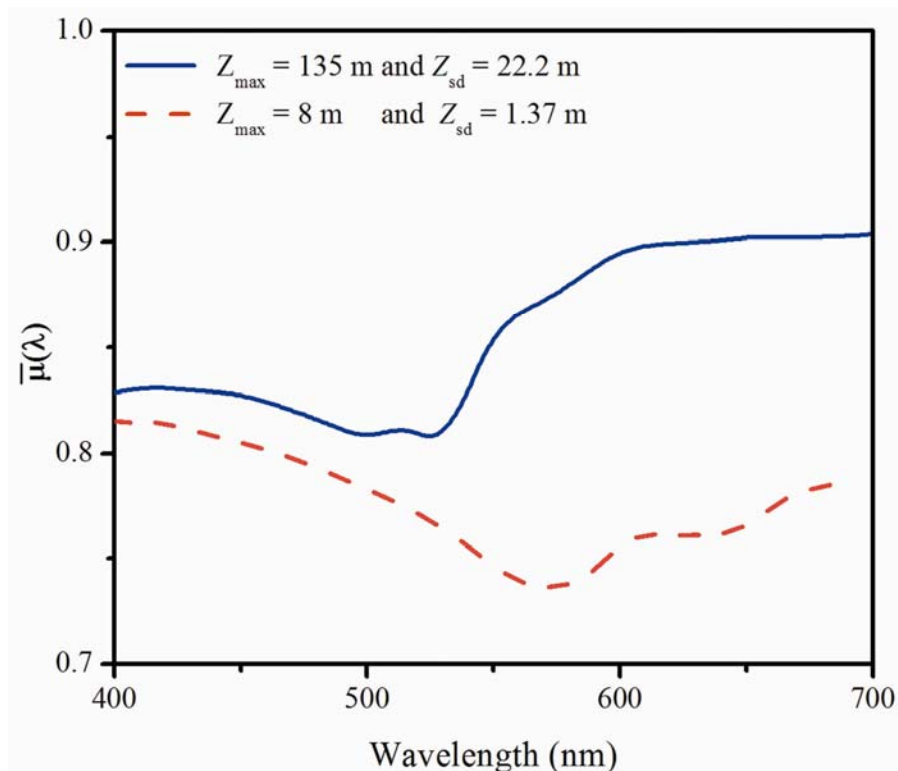


Figure 5 Spectral underwater average cosines for various water types.

The spectral variations in  $\bar{\mu}$  depends on phase function and single scattering albedo ( $\omega_0$ ), which is defined as the ratio of scattering coefficient ( $b$ ) to the beam attenuation coefficient ( $c$ ) ( $\omega_0 = b/c$ ) (Haltrin 2000; Berwald et al. 1995). Its spectral shape can be well explained with respect to absorption and scattering coefficients. The absorption of blue band by Colored Dissolved Organic Matter (CDOM) and detritus dominates over the scattering of green band, giving high values to  $\bar{\mu}(\lambda)$  in blue band as compared to in green band. Similarly, the dominance of absorption of red band by phytoplankton over scattering gives higher values to  $\bar{\mu}(\lambda)$  for both water types. The large difference between values of  $\bar{\mu}(\lambda)$  in red band for coastal and relatively clearer waters could be attributed to the degree of dominance of absorption over scattering in this region for the two water types.

Figure 6 shows the spectral variation of  $\omega_0(\lambda)$  and  $\bar{\mu}(\lambda)$  for three different water types.  $\omega_0(\lambda)$  and  $\bar{\mu}(\lambda)$  are found to vary inversely with each other. Higher values of  $\omega_0(\lambda)$  (approaching 1) indicate dominance of scattering thus widening the underwater radiance distribution and resulting in reduced  $\bar{\mu}(\lambda)$  whereas the lower values of  $\omega_0(\lambda)$  (approaching 0) indicate the dominance of absorption over scattering thus restricting the radiance to travel in single direction and hence increasing  $\bar{\mu}(\lambda)$  (Berwald 1998). We also observed the similar relations between  $\bar{\mu}(\lambda)$  with  $b(\lambda)/a(\lambda)$  as observed by Kirk (1981) (Figure 7). The values of  $\bar{\mu}(\lambda)$  are found to decrease with increasing contribution of scattering relative to absorption.

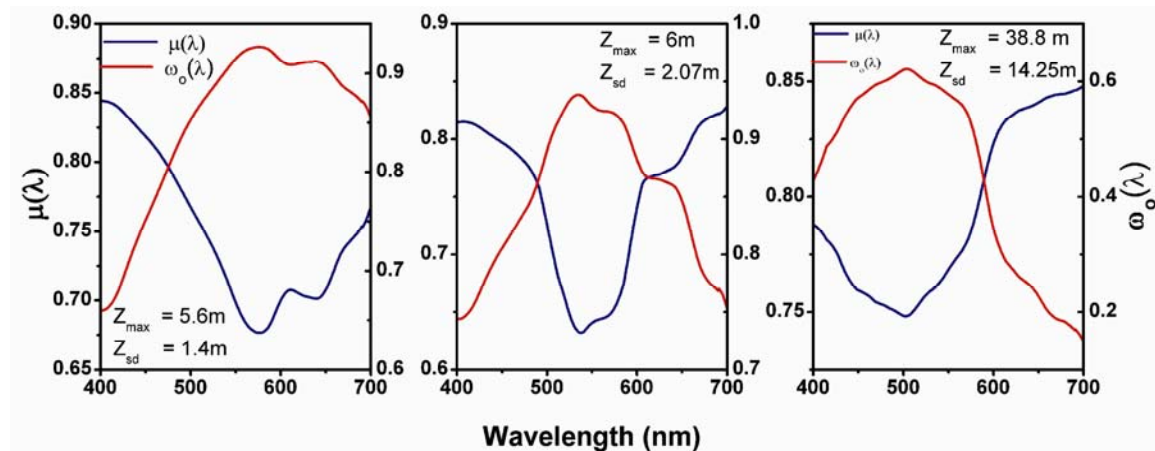


Figure 6 Spectral variations of  $\omega_0(\lambda)$  and  $\bar{\mu}(\lambda)$  obtained from Hydrolight for different water types

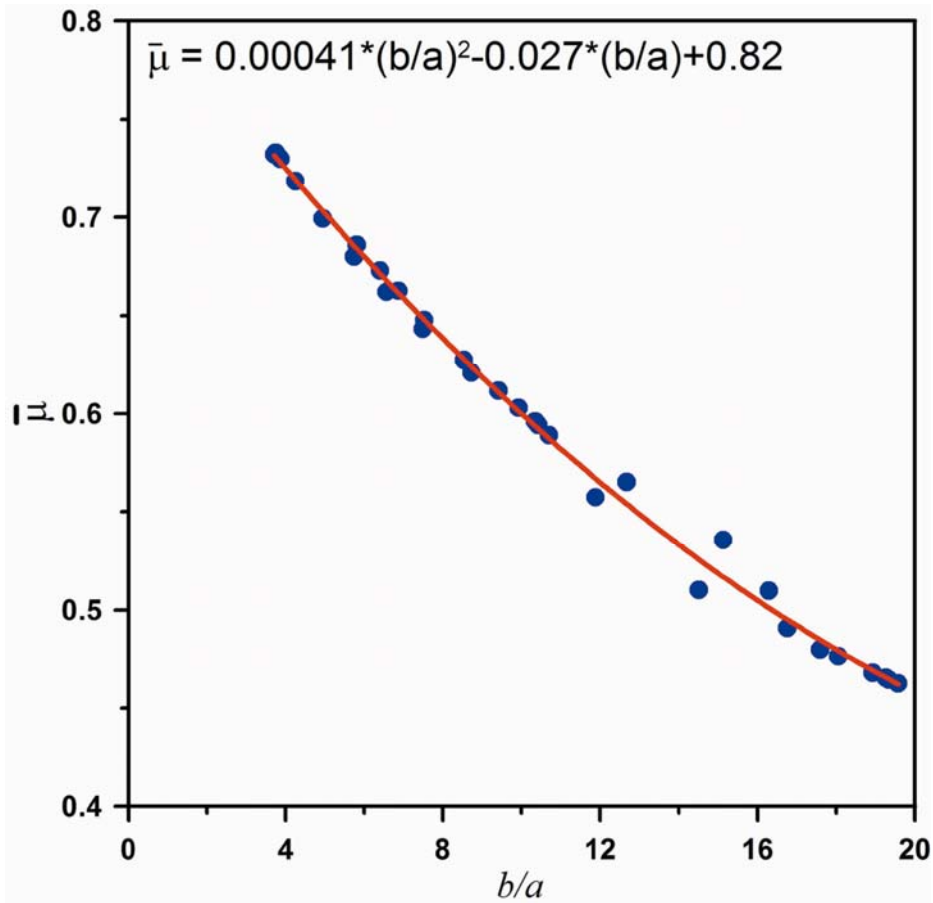


Figure 7 Variations of  $\bar{\mu}$  with  $b/a$  obtained from Hydrolight

#### *Underwater average cosine profile*

Depth profiles of underwater average cosine are important for understanding the underwater light field. It is also one of the key parameters for estimation of primary productivity. The vertical behavior of underwater average cosine in vertically homogenous medium with flat surface has been studied by Kirk (1981), Zaneveld (1989), Bannister (1992), McCormick (1995) and Berwald et al. (1995, 1998). Depth variation of  $\bar{\mu}(490)$  nm shows strong relationship with ratio of scattering to absorption at 490nm (Figure 8). For deeper depths dominance of scattering over absorption broadens the radiance distribution thus reducing  $\bar{\mu}(\lambda)$ . Rapid increase in value of  $b/a$  at 490nm, increases the rate of change of  $\bar{\mu}(490)$  with depth. This agrees with the findings of Berwald et al. (1995), indicating that the rate of change of  $\bar{\mu}$  with depth is dependent more on scattering than absorption.

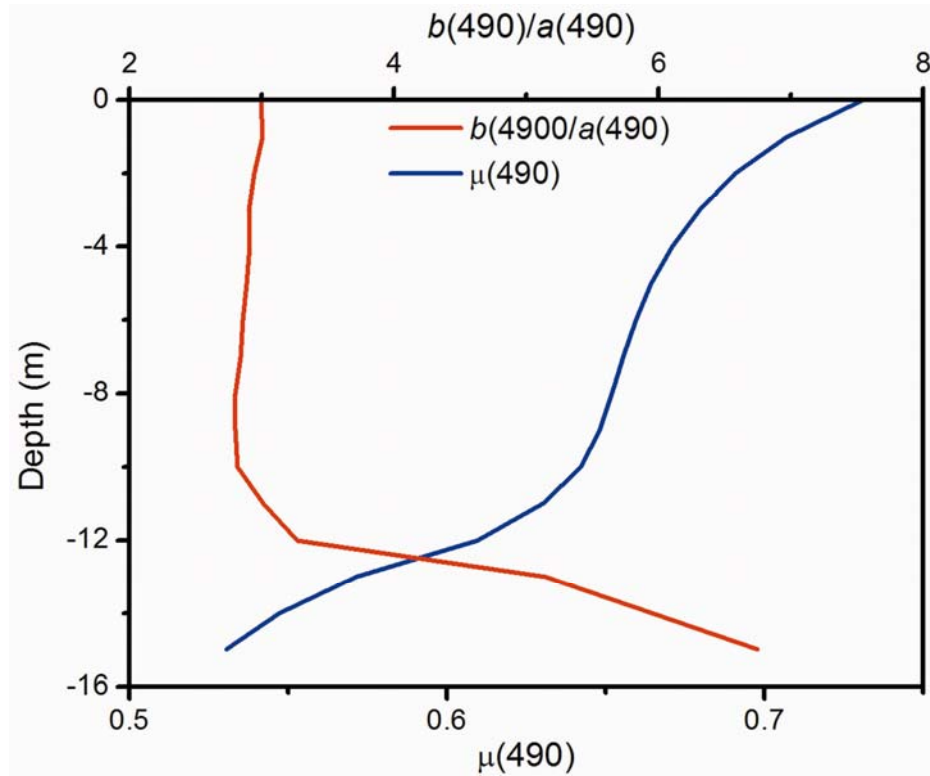


Figure 8 Variation of  $\mu(490)$  and  $b(490)/a(490)$  with depth. The variations were similar to that obtained by Kirk (1981).

#### *Assessment of algorithms*

The values of  $\bar{\mu}(\lambda)$  derived from algorithms Mu, Haltrin and Timofeyeva using the measured  $R_{rs}(\lambda)$  were compared with those derived from the Hydrolight simulations. The algorithm Mu performed better than the other two algorithms of Haltrin and Timofeyeva with lower values of RMSE, APD and MPD and coefficient of determination greater than 0.8 for all spectral regions (Figure 9, 10, Table 2). The  $\bar{\mu}(\lambda)$  derived using algorithms of Haltrin and Timofeyeva were overestimated. Figure 10 show the  $\bar{\mu}(\lambda)$  derived using all the algorithms for two different water types. The relative difference (Figure 11) plotted for these water types shows that the algorithm Mu performed well for all water types.

Table 2 Evaluation of algorithms Mu, Haltrin and Timofeyeva using the measured remote sensing reflectance

	RMSE	APD	MPD	R <sup>2</sup>
<b>For all bands</b>				
<b>Mu</b>	0.028	0.031	0.125	0.86
<b>Haltrin</b>	0.044	0.047	3.347	0.78
<b>Timofeyeva</b>	0.061	0.070	2.645	0.76
<b>For blue region</b>				
<b>Mu</b>	0.026	0.029	0.114	0.79
<b>Haltrin</b>	0.043	0.046	2.912	0.69
<b>Timofeyeva</b>	0.059	0.064	3.508	0.68
<b>For green region</b>				
<b>Mu</b>	0.028	0.033	0.132	0.87
<b>Haltrin</b>	0.037	0.043	2.895	0.82
<b>Timofeyeva</b>	0.054	0.068	0.189	0.79
<b>For red region</b>				
<b>Mu</b>	0.029	0.031	0.128	0.83
<b>Haltrin</b>	0.051	0.053	4.225	0.74
<b>Timofeyeva</b>	0.071	0.076	4.224	0.71

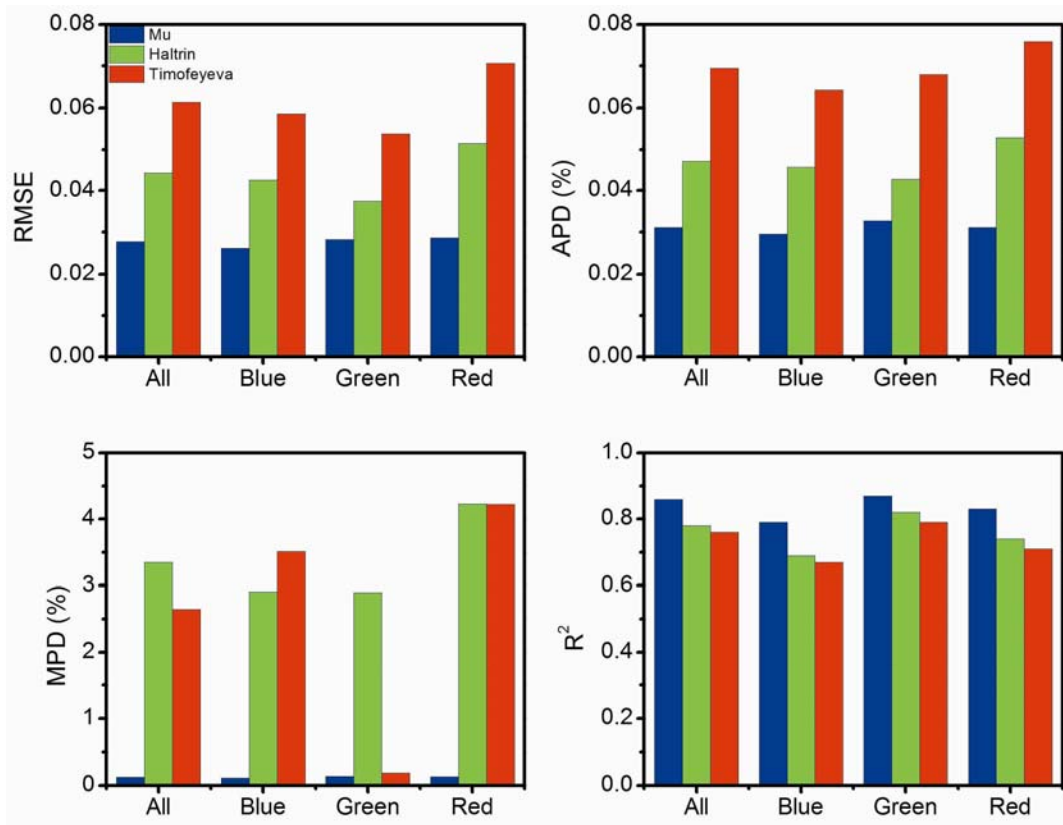


Figure 9 Error analysis of the algorithms Mu(Blue), Haltrin(Green) and Timofeyeva(Red) using in-situ measured  $R_{rs}(\lambda)$



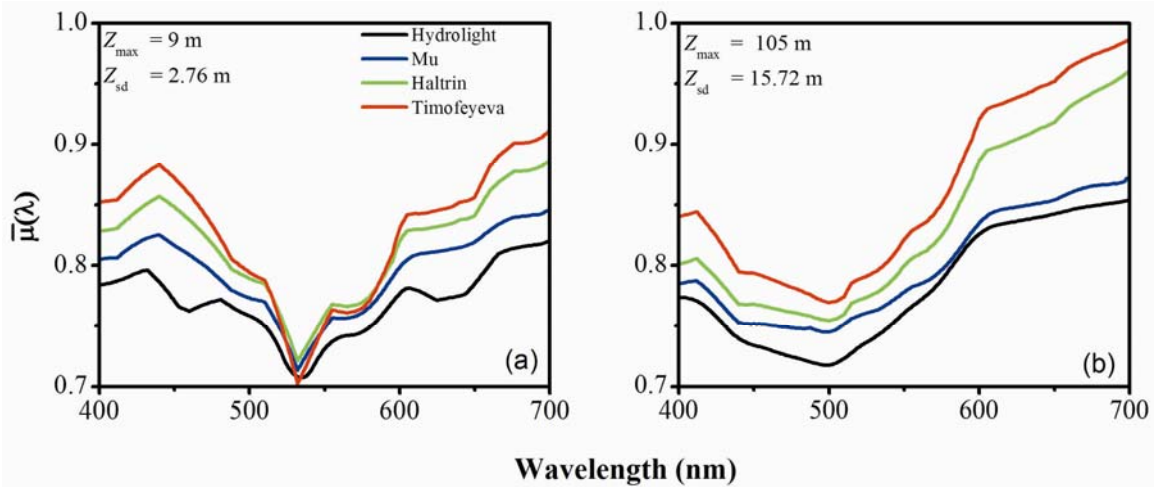


Figure 10 Comparison of  $\mu(\lambda)$  derived from Hydrolight (Black) with those obtained from measured remote sensing reflectance using algorithms, Mu (Blue), Haltrin (Green) and Timofeyeva (Red)

Spectral variations of  $\bar{\mu}(\lambda)$  for the two water types show distinct features at blue, green and red regions (Figure 10). For the coastal waters (Figure 10a) there was a symmetric variation about the green region which has very low values and high values on either side in the blue and red. For the clearer water (Figure 10b), the values were relatively higher in the red region compared to blue and green. For both water types the lowest values were found in the green region. The spectral variations with higher values in the blue and red were due to the dominance of absorption to scattering and the low values in green were due to dominance of scattering with low absorption. Although all the algorithms show similar spectral variations, the Mu was found to score over other algorithms in all spectral regions and for both the water types. The closest match for all algorithms was found in the green region and the largest deviation in the red region. The largest differences over the complete spectral range for both water types were observed for Timofeyeva. (Figure 11)

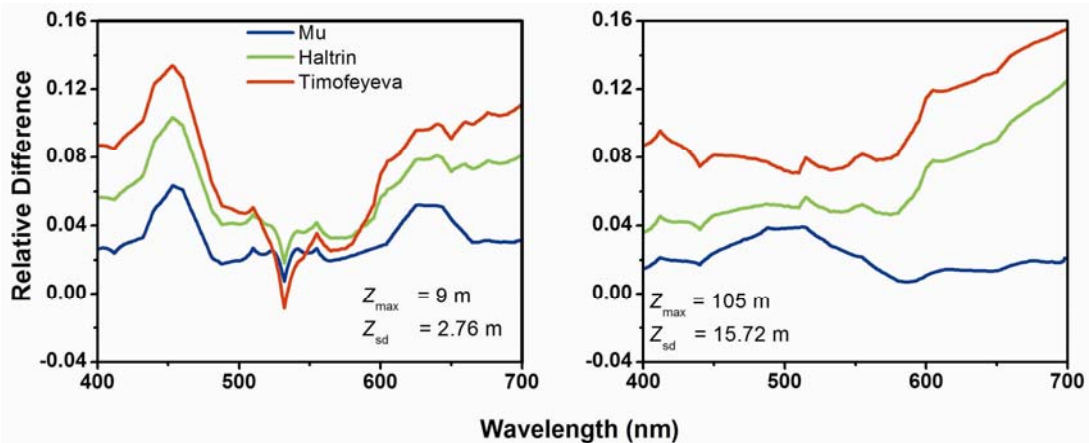


Figure 11 Relative differences between the  $\mu(\lambda)$  calculated using all the algorithms and values of  $\mu(\lambda)$  generated from Hydrolight for two different water types.

## Discussion

The radiative transfer model Hydrolight version 5.1 was used for simulating the measured optical properties. Although the simulations were carried-out with the measured input parameters and minimizing the assumptions and empirical relations for any parameters, the radiative transfer simulations could have been more rigorous considering various factors not included in our study. In our study the surface and bottom boundary conditions were assumed to be flat, surface of water was assumed to be flat and did not include the effects of wavy surface and also inelastic scattering. Some of these problems have been addressed and will need to be studied later (Sunderabalan and Shanmugham 2013). Since the measurements on phase function were not available, the phase function was assumed to be constant throughout the depth.

The algorithm was validated using the remote sensing reflectance measured using hyperspectral radiometer and was also compared with the two algorithms of Haltrin and Timofeyeva. The two algorithms uses inherent optical properties such as absorption, scattering, beam attenuation and back scattering coefficients and they were developed to be used in both open as well as coastal oceanic waters for deriving underwater average cosine for full spectral range. The algorithm Mu performed much better than these two algorithms for both turbid as well as relatively clear waters.

The underwater average cosine is a much sought after optical parameter that will help in better understanding of behavior of light in water. However, presently there are no commercial instruments available to obtain this parameter. Some algorithms to derive average cosine have been developed for specific bands or specific wavelengths valid for specific boundary conditions (Berwald et al. 1995; Stramska et al. 2000; Talaulikar et al. 2012) while others assume average cosine to be a constant value (Ciotti et al.1999; Penta et al. 2008), however it was observed to vary spectrally. Hence, assuming a constant value will yield erroneous results in models and related applications for the waters with varying absorption and scattering properties. The present algorithm was found to be valid for the spectral range 400-700nm and it has been validated for various water types and wide range of values. Since the present algorithm provides spectral values it could be used to derive spectral optical properties such as absorption.

Presently there are no algorithms available to compute spectral  $\bar{\mu}(\lambda)$  from satellite data and since this algorithm computes spectral  $\bar{\mu}(\lambda)$  based on  $R_{rs}(\lambda)$ , it is well suited for ocean color

applications. Unlike the earlier reported algorithms of Haltrin (1998, 2000) the present algorithm has the advantage that it does not depend on the inherent optical properties.

The inter-comparisons of reported algorithms with the present algorithm show vast improvements in performance compared to other algorithms (Table 2) due to ease of implementation with fewer parameters. The algorithm showed consistency in performance over the entire spectral range unlike other algorithms which showed larger deviations in the lower and higher range of wavelengths and close match only around 500 nm (Figure 10 and 11). Algorithms of Haltrin and Timofeyeva were found to overestimate  $\bar{\mu}(\lambda)$ .

### **Comments and recommendations**

Because the algorithm  $\mu$  depends on just one optical parameter  $R_{rs}(\lambda)$  it could be used to determine the mean cosine from all ocean color satellite sensors. However, the performance of the algorithm will depend on the values of  $R_{rs}(\lambda)$  and hence a robust atmospheric correction algorithm will be required for the ocean color satellite (Shanmugam 2012; Shanmugam et al. 2013).

The spectral absorption coefficient  $a(\lambda)$  can be determined using  $\bar{\mu}(\lambda)$  and  $K_d(\lambda)$ . The exact equation for diffuse attenuation coefficient for downwelling irradiance  $K_d(\lambda)$  can be approximated under certain conditions such as subsurface reflectance  $R \ll 1$ , Case1 or CDOM dominated waters and assuming  $K_d \approx K_u$ , then  $a(\lambda) \sim \bar{\mu}(\lambda) K_d(\lambda)$  (Gordon, 1989). Using the conservation of energy, Gershun (1939) provided a relationship to derive inherent optical property,  $a(\lambda) = \bar{\mu}(\lambda) K_E(\lambda)$ , where the diffuse attenuation coefficient for net or vector irradiance,  $K_E(\lambda)$  is approximated to  $K_d(\lambda)$  under some assumptions and the same was also observed in our data. (Kirk 1981; Morel 1991; Sokoletsky et al. 2003; Darecki et al. 2003). There are several algorithms available for deriving  $K_d(\lambda)$  from ocean color satellite sensors, which have been evaluated for the study area by Suresh et al. (2012). The average cosine of underwater light field varies with different water types as it is influenced by scattering and absorption and thus can be used for classifying the water types and perhaps to develop an empirical algorithm to determine the transparency of water.

The present algorithm could be improved based on a depth factor to extend the remotely derived average cosine property in order to obtain the depth profiles of underwater light field in coastal waters.

## **Acknowledgement**

We are thankful to the Director of National Institute of Oceanography (NIO) and Indian National Centre for Ocean Information Services (INCOIS) for the support. The study was carried-out under project SATCORE (Satellite Coastal and Oceanographic Research) funded by INCOIS. We are also thankful to Dr. Juli Berwald for her valuable suggestions. Authors are also thankful to the colleagues who rendered their help in measurement of data and preparation of manuscript and the reviewers whose valuable comments helped in improving this manuscript. The first author also thanks CSIR (Council of Scientific and Industrial Research, New Delhi) for awarding the Senior Research Fellowship (SRF).

## **References:**

- Bannister, T. T. 1992. Model of the mean cosine of underwater radiance and estimation of underwater scalar irradiance. *Limnology And Oceanography*. 37:773-780.
- Berwald, J. 1998. Relationship between the average cosine of the underwater light field and the inherent optical properties of the ocean. PhD thesis. University of Southern California.
- Berwald, J., Stramski, D., Mobley, C. D., And Kiefer, D. A. 1995. Influences of absorption and scattering on vertical changes in the average cosine of the underwater light field. *Limnology And Oceanography*. 40:1347–1357.
- Berwald, J., Stramski, D., Mobley, C. D., and Kiefer, D. A. 1998. Effect of Raman scattering on the average cosine and diffuse attenuation coefficient of irradiance in the ocean. *Limnology And Oceanography*. 43:564-576.
- Ciotti, A. M., Cullen, J. J. and Lewis, M. R. 1999. A semi-analytical model of the influence of phytoplankton community structure on the relationship between light attenuation and ocean color, *J. Geophys. Res.*, 104:1559–1578.
- Darecki, M., Weeks, A., Sagan, S., Kowalczyk, P. and Kaczmarek, S. 2003. Optical characteristics of two contrasting Case 2 waters and their influence on remote sensing algorithms. *Cont Shelf Res*. 23(3-4):237–250.
- Fournier, G. and Forand, J. L. 1994. Analytic phase function for ocean water. *Ocean Optics XII*. J. S. Jaffe, ed., Proc. SPIE 2258, 194.
- Gallegos, C. and Correll, D. 1990. Modeling spectral diffuse attenuation, absorption and scattering coefficients in a turbid estuary. *Limnology and Oceanography*. 35(7):1486-1502.
- Gershun, A. A. 1939. The lightfield. *Journal of Mathematical Physics*. 18:51-151.
- Gordon, H. 1989. Theoretical aspects of hydrologic optics. *Limnology and Oceanography*. 34(8):1389–1409.

- Gordon, H.R. and Clark, D.K. 1980. Remote sensing optical properties of a stratified ocean: an improved interpretation. *Appl. Opt.*,19,3428-3430.
- Gordon, H.R. and Morel, A. 1983. Remote assessment of ocean color for interpretation of satellite visible imagery: A review. New York: Springer-Verlag. 114.
- Gould, R. W. Arnone, Jr. R. A., Sydor, M. 2001. Absorption, scattering, and remote sensing reflectance relationships in coastal waters: Testing a new inversion algorithm. *17(2)*:328-341.
- Gould, R. W. Arnone, Jr. R. A., Martinolich, P. M. 1999. Spectral dependence of the scattering coefficient in case 1 and case 2 waters. *Applied Optics*. 38(12):2377-83
- Haltrin, V. I. 1998. Self-consistent approach to the solution of the light transfer problem for irradiances in marine waters with arbitrary turbidity, depth, and surface illumination. I. Case of absorption and elastic scattering. *Applied Optics*. 37: 3773– 3784.
- Haltrin. V. I. 2000. Empirical algorithms to restore a complete set of inherent optical properties of seawater using any two of these properties. *Canadian Journal Of Remote Sensing*. 26(5):440-445.
- Hojerslev, N. K. And Zaneveld, J. R. V. 1977. A theoretical proof of the existence of the submarine asymptotic daylight field. *University Copenhagen Oceanography Series*. 34:16.
- Hojerslev, N.K. 1973. Inherent and apparent optical properties of the western Mediterranean and the Hardangerfjord. *Univ. Copenhagen, Inst. Phy. Oceanogr. Rep.*21-23
- Kirk, J. T. O. 1981. Monte Carlo study of the nature of the underwater light field in and the relationships between optical properties of turbid yellow waters. *Australian Journal of Marine & Freshwater Research*. 32:517-532.
- Kirk, J. T. O. 1994. *Light and photosynthesis in aquatic ecosystems*. 2<sup>nd</sup> Ed. (Cambridge : Cambridge University Press).
- Lee, Z. P., A. Weidemann, J. Kindle, R. Arnone, K.L. Carder, C. Davis. 2007. Euphotic zone depth: Its derivation and implication to ocean-color remote sensing. *J. Geophys. Res.*, 112, C03009, doi:10.1029/2006JC003802.
- Lee, Z. P., Carder, K. L., Arnone, R., 2002. Deriving inherent optical properties from water color: a multi-band quasi-analytical algorithm for optically deep waters. *Appl. Opt.*, 41, 5755-5772.
- Lee, Z. P., K. L. Carder, C. D. Mobley, R. G. Steward, and J. S. Patch. 1999. 1. Hyperspectral remote sensing for shallow waters. 2. Deriving bottom depths and water properties by optimization. *Appl. Opt.*, 38, 3831–3843.
- Loisel, H., & Stramski, D. 2000. Estimation of the inherent optical properties of natural waters from the irradiance attenuation coefficient and reflectance in the presence of Raman scattering. *Applied optics*. 39(18):3001–11.

- McCormic, N. J. 1995. Mathematical models for the mean cosine of irradiance and the diffuse attenuation coefficient. *Limnology and Oceanography*. 40:1013 -1018.
- Mobley, C. D. 1994. *Light and water: radiative transfer in natural waters*. Academic Press.
- Mobley, C. D., Sundman, L. K., & Boss, E. 2002. Phase function effects on oceanic light fields. *Applied optics*. 41(6): 1035–50.
- Morel, A. 1991. Light and marine photosynthesis: a spectral model with geochemical and climatological implications. *Prog Oceanogr*. 26:263–306.
- Pegau, W.S., D. Gray, and J. R. V. Zaneveld. 1997. Absorption and attenuation of visible and near-infrared light in water: dependence on temperature and salinity. *Appl. Opt.*,36,6035-6046.
- Pelevin, V. N., and Prokudina, T. M. 1979. On the relation of parameters of deep radiance distribution upon p criterion in light fields in the ocean. Institute Of Oceanology, Academy of Sciences of The USSR, Moscow. pp. 34–38.
- Penta, B., Z. Lee, R. M. Kudela, S. L. Palacios, D. J. Gray, J. K. Jolliff, and I. G. Shulman. 2008. An underwater light attenuation scheme for marine ecosystem models. *Optics Express*. 16:16581-16591.
- Petzold, T. J. 1972. Volume scattering functions for selected ocean waters. Scripps Institution of Oceanography, Report SI0. pp. 72–78.
- Preisendorfer, R. W. 1959. Theoretical proof of the existence of characteristic diffuse light in natural waters. *Journal of Marine Research*.18:1-9.
- Qin, Y., V. E. Brando, A. G. Dekker, and D. Blondeau-Patissier. 2007. Validity of SeaDAS water constituents retrieval algorithms in Australian tropical coastal waters. *Geophys. Res. Lett.* 34
- Sathyendranath, S., and Platt, T. 1989. Computation of aquatic primary production: extended formalism to include effect of angular and spectral distribution of light. *Limnology and Oceanography*. 34:188-198.
- Shanmugam, P., 2012. CAAS: an atmospheric correction algorithm for the remote sensing of complex waters. *Annales Geophysicae*. 30:203–220.
- Shanmugam, P., Ahn, Y. H., Ryu, J. H., Sundarabalan, V. B. 2010. An evaluation of inversion models for retrieval of inherent optical properties from ocean color in coastal and open sea waters around Korea. *Journal of Oceanography*. 66:815–30.
- Shanmugam, P., Suresh, M. and Sundarabalan, V., B. 2013. OSABT: An innovative algorithm for characterization of ocean surface algal blooms in oceanic waters around India. *IEEE Journal of Selected Topics in Applied Earth Observations and Remote Sensing*. 6(4): 1879-1892.

- Sokoletsky, L., Dubinsky, Z., Shoshany, M. & Stambler, N. 2003. Estimation of phytoplankton pigment concentration in the Gulf of Aqaba (Eilat) by in situ and remote sensing single-wavelength algorithms. *International Journal of Remote Sensing*. 24(24):5049-5073
- Stramska, M., Stramski, D., Greg M. B., Mobley, C. D. 2000. Estimation of the absorption and backscattering coefficients from in-water radiometric measurements. *Limnology and Oceanography*. 45:628–641.
- Suresh T., Talaulikar, M., Desa, E., Matondkar, S.G.P. & Antonio Mascarenhas. 2012. Comparison of measured and satellite-derived spectral diffuse attenuation coefficients for the Arabian Sea. *International Journal of Remote Sensing*. 33(2): 570-585.
- Talaulikar, M., T. Suresh, E. Desa, S. G. P. Matondkar, T. Srinivasa Kumar, A. Lotliker, A. B. Inamdar. 2011. Empirical algorithm to estimate the average cosine of underwater light field at 490 nm. *Remote sensing letters*, 3(7): 585 – 593.
- Timofeyeva, V. A. 1971. Optical characteristics of turbid media of the seawater type. *Izvestiya Atmospheric and Oceanic Physics*, 7:863-865.
- V. B. Sundarabalan, and Shanmugam, P. 2013. Radiative transfer modeling of upwelling light fields in coastal waters. *Journal of Quantitative Spectroscopy and Radiative Transfer*, 121, 30-44.
- Zaneveld, J. R. 1989. An asymptotic closure theory for irradiance in the sea and its inversion to obtain the inherent optical properties. *Limnology and Oceanography*. 34:1442-1452.
- Zaneveld, J. R. V., J. C. Kitchen and C. M. Moore. 1994. The scattering error correction of reflecting-tube absorption meters. *Proc. SPIE* 2258, 44-55.